Published in final edited form as:
Nat Geosci. 2019 ; DEC 2019: . doi:10.1038/s41561-019-0492-6.

Great Oxidation and Lomagundi events linked by deep cycling and enhanced degassing of carbon

James Eguchi[1,2], **Johnny Seales**[1], **Rajdeep Dasgupta**[1]

[1]Department of Earth, Environmental and Planetary Sciences, Rice University, 6100 Main Street, MS-126, Houston, TX 77005

[2]Current Address: Department of Earth and Planetary Sciences, University of California, Riverside, 900 University Ave., Riverside, CA 92521

Abstract

For approximately the first 2 billion years of Earth history, atmospheric oxygen levels were extremely low. It wasn't until at least half a billion years after the evolution of oxygenic photosynthesis, perhaps as early as 3 billion years ago, that oxygen rose to appreciable levels during the Great Oxidation event. Shortly after, marine carbonates experienced a large positive spike in carbon isotope ratios known as the Lomagundi event. The mechanisms responsible for the Great Oxidation and Lomagundi events remain debated. Using a carbon-oxygen box model which tracks surface and interior C fluxes and reservoirs while also tracking C isotopes and atmospheric oxygen levels we demonstrate that about 2.5 billion years ago a tectonic transition resulting in increased volcanic CO_2 emissions could have led to increased deposition of both carbonates and organic carbon via enhanced weathering and nutrient delivery to oceans. Increased burial of carbonates and organic carbon would have allowed accumulation of atmospheric oxygen while also increasing delivery of carbon to subduction zones. Coupled with preferential release of

Corresponding Author: James Eguchi, eguchi.james@gmail.com.

Author contributions

J.E. conceived the project, compiled necessary data and developed the model as part of his PhD thesis. J.S. helped develop the box model and provided insight on geodynamic considerations. R.D. guided J.E. as his thesis advisor to help refine the idea. All authors contributed to writing of the manuscript.

Competing financial interests

The authors declare no competing financial interests.

Data Availability

Data used in the generation of Fig. 1 were taken directly without any alteration from the references given in the figure caption and can be accessed in the original publications cited in the figure caption. Additionally the original author has made the data compilation of C isotopes available on his personal website: http://www.krisstott.com/publications.html. Data used in Fig. 2a is reported in Supplementary Table 2 and can be accessed from the original publications cited in the table. Additionally, the data in Supplementary Table 2 has been made publicly available at earthchem.org (DOI:10.1594/IEDA/111406). Compiled data used in Fig. 3 is reported in Supplementary Table 3 and can be accessed from the original publications cited in the table. Additionally, the data in Supplementary Table 3 has been made publicly available at earthchem.org (DOI:10.1594/IEDA/111406).

Code Availability

All equations required by the model are presented in the methods section. The python code for the model is included in the online supplementary material, and is available online at https://github.com/jameseguchi.

Additional information

Supplementary information is available in the online version of the paper. Reprints and permissions information is available online at www.nature.com/reprints.

carbonates at arc volcanoes and deep recycling of organic C to ocean island volcanoes we find such a tectonic transition can simultaneously explain the Great Oxidation and Lomagundi events without any change in the fraction of carbon buried as organic carbon relative to carbonate, which is often invoked to explain carbon isotope excursions.

Carbon dioxide and oxygen, two gases critical for Earth's habitability, are linked via photosynthesis:

$$CO_2 + H_2O = CH_2O + O_2 \quad (1)$$

The link between CO_2 and O_2 is evident in the geologic record from the association of the most dramatic events in the histories of both gases. The Great Oxidation Event (GOE), during which Earth's atmospheric oxygen levels increased by several orders of magnitude, and the Lomagundi Event (LE), during which carbon isotope ratios of marine carbonates increased by up to ~10‰, both occurred around 2.3–2.0 Ga[1–3] (Fig. 1). The temporal association of the two events suggests both may be attributed to a single mechanism, such as enhanced organic carbon burial[4]. This is because increasing the fraction of carbon buried as organic carbon (f_{org}) relative to carbonate will increase the amount of oxygen produced and allowed to accumulate via equation (1). Increased f_{org} also increases $\delta^{13}C$ of carbonates because organic matter preferentially incorporates ^{12}C, leaving the carbonate-forming C reservoir enriched in ^{13}C (ref. [4]).

Despite the apparent temporal association of the GOE and LE and the conceptual consistency of explaining both events via increased f_{org}, its role as the driver of the GOE and LE has been questioned. There is evidence that oxygenic photosynthesis evolved at least half a billion years before the GOE[5], so why would atmospheric oxygen have remained low for so long?[6]. In addition, other studies have suggested that the GOE may have preceded the LE by ~100 million years[2,3,7,8]. If the onset of the GOE and LE were indeed temporally disparate, it becomes difficult to explain both events via a single mechanism. This has led researchers to propose mechanisms invoking decreased sinks of atmospheric oxygen as the main driver of the GOE[9–11]. While decreased oxygen sinks would allow atmospheric O_2 to accumulate, it is unclear how they would drive the associated positive C isotope excursion.

Here, we propose a single mechanism for the GOE and LE. Our modeling shows that the proposed mechanism can simultaneously explain increased oxygen production as well as a positive C isotope excursion in marine carbonates. In addition, we show that the proposed mechanism is consistent with a delay between the evolution of photosynthesis and increased atmospheric oxygen levels, as well as a delay between the build-up of oxygen in the atmosphere and the positive C isotope excursion observed in marine carbonates.

Enhanced volcanic CO_2 driven by tectonic transitions

We propose that around 2.5 billion years ago a major tectonic transition increased volcanic CO_2 emissions, driving increased rates carbonate and organic C burial via enhanced weathering and nutrient delivery to oceans. A transition from stagnant/sluggish lid to plate tectonics has been proposed around 2.5 Ga[12], which would have caused increased volcanic

CO_2 emissions[13,14]. Also proposed around 2.5 billion years ago are the rapid emergence of subaerial continents[15] and major glaciations[16]. These events would have increased the supply of hydrated sediments to trenches, lubricating the subduction interface and enhancing plate tectonic activity, which would have led to enhanced volcanic CO_2 emissions[17]. Moussallam et al.[18] propose that mantle cooling resulted in lower eruptive temperatures for volcanic gases, which caused the gases to become more oxidized, resulting in CO_2 emissions to increase relative to emissions of more reduced C gases.

A GOE resulting from tectonically-driven increases in volcanic CO_2 emissions is consistent with oxygenic photosynthesis evolving prior to the GOE[5] because the production rate of oxygen is controlled by the flux of organic C burial:

$$F_{org} = F_{tot} \times f_{org} \quad (2)$$

where F_{org} is the flux of organic carbon burial, and F_{tot} is the flux of total carbon burial (carbonate + organic C). Therefore, F_{org}, and the oxygen production flux, can increase by increasing F_{tot}, instead of f_{org}. At the onset of oxygenic photosynthesis, oxygen production could have been low because Earth's tectonic mode promoted low weathering fluxes (*i.e.*, stagnant-lid, un-emerged continents), resulting in low F_{tot} and thus low F_{org}. Then a tectonic transition could have increased F_{tot} and thus F_{org}, resulting in a delay between the evolution of photosynthesis and the GOE[5,19]. This could have all been achieved without any significant changes to f_{org}.

Carbonate release at arcs drive positive spike in $\delta^{13}C$

Positive $\delta^{13}C$ excursions in carbonates are commonly attributed to increased f_{org}:

$$\delta^{13}C_{in} = \delta^{13}C_{carb}(1 - f_{org}) + \delta^{13}C_{org} f_{org} \quad (3)$$

where $\delta^{13}C_{in}$ is $\delta^{13}C$ of atmospheric inputs of CO_2 and $\delta^{13}C_{org}$ is $\delta^{13}C$ of organic C. If fractionation of C isotopes between carbonates and organic C ($\Delta^{13}C_{carb\text{-}org} \equiv \delta^{13}C_{carb} - \delta^{13}C_{org} \approx 25‰$), and $\delta^{13}C_{in}$ remain constant, increased f_{org} increases $\delta^{13}C_{carb}$. $\delta^{13}C_{carb}$ also increases if $\delta^{13}C_{in}$ increases at constant f_{org} and $\Delta^{13}C_{carb\text{-}org}$. We propose that the increased $\delta^{13}C_{carb}$ of the LE could have been caused by increased $\delta^{13}C_{in}$ rather than increased f_{org}.

$\delta^{13}C_{in}$ depends on the balance of CO_2 being emitted at different volcanic settings:

$$\delta^{13}C_{in} = \frac{F_{OIB}}{F_{tot}}\delta^{13}C_{OIB} + \frac{F_{MORB}}{F_{tot}}\delta^{13}C_{MORB} + \frac{F_{arc}}{F_{tot}}\delta^{13}C_{arc} \quad (4)$$

where F_i is CO_2 flux at volcanic setting i and $\delta^{13}C_i$ is $\delta^{13}C$ of CO_2 emitted at volcanic setting i. $\delta^{13}C_{MORB} \approx -5‰$[20,21], CO_2 flux-weighted $\delta^{13}C_{arc} \approx -3‰$[22], and sparse studies on $\delta^{13}C_{OIB}$ suggest it could be similar to MORB or more negative[21,23]. Therefore, increasing $\frac{F_{arc}}{F_{tot}}$ increases $\delta^{13}C_{in}$ by shifting the balance of $\delta^{13}C_{in}$ towards $\delta^{13}C_{arc}$.

The tectonic transitions discussed above can increase carbonate and organic C burial leading to increased subduction of C. Upon reaching subarc depths the increased flux of subducted C would be released from the slab at an increased rate resulting in increased $\frac{F_{arc}}{F_{tot}}$, shifting the balance of $\delta^{13}C_{in}$ towards $\delta^{13}C_{arc}$. This mechanism is consistent with oxygenation preceding increased $\delta^{13}C_{carb}$[8] because oxygen accumulates immediately after burial of organic C. Contrastingly, $\delta^{13}C_{carb}$ increases after the increased C flux is buried, subducted, released from the slab, emitted at arcs as CO_2, and incorporated into marine carbonates. Evidence for increased delivery of subducted sediments to arc volcanic sources is provided by the record of covariance of $\delta^{18}O$ and εHf in zircons - both of which quantify the contribution of subducted weathering products to magma generation[24]. Fig 1c shows that the peak in $\delta^{13}C_{carb}$ closely correlates with the peak in $\delta^{18}O$-εHf_{zircon} covariance, supporting the idea that $\delta^{13}C_{carb}$ may be controlled by the balance of $\delta^{13}C$ of CO_2 emitted at different volcanic centers.

Increasing $\delta^{13}C_{in}$ by increasing $\frac{F_{arc}}{F_{tot}}$ is possible if $\delta^{13}C_{arc}$ is high, which is most easily explained by a heavy contribution of carbonates to arc CO_2 emissions. A recent study determined that the flux-weighted, average $\delta^{13}C_{arc} \approx -3‰$[22]. Whether high $\delta^{13}C_{arc}$ is due to contribution of carbonates from the subducted slab or upper crust remains debated[22,25]. Figure 2a shows $\delta^{13}C_{arc}$ versus f_{org} of the sediments entering the respective trench. As f_{org} of subducted C becomes greater, $\delta^{13}C_{arc}$ becomes more negative, implying that f_{org} of subducted sediments is the dominant controller of $\delta^{13}C_{arc}$[26]. The dashed line in Fig. 2a shows what $\delta^{13}C_{arc}$ would be if carbonates and organic C were released with equal efficiency. Data in Fig. 2a suggest preferential carbonate release, supporting the idea that $\delta^{13}C_{arc}$ is high due to preferential release of carbonates relative to organic C from the subducted slab. Below, we test whether ancient arcs may have also had high $\delta^{13}C$.

Ancient subduction zones were likely hotter than present day due to secular mantle cooling[27]. Figure 2b,c demonstrates that along *P-T* paths of subducting slabs adjusted for secular mantle cooling[27], carbonate will be removed from the slab more efficiently than organic C, which metamorphoses to graphite during subduction[28]. In a carbonated pelitic sediment, metamorphic decarbonation and partial melting[29] can release up to 100% of subducted carbonates (Fig. 2c). Graphite removal via CO_2 dissolution in pelitic sediment partial melts can only extract up to ~50% of the subducted organic C. This demonstrates that like present-day arcs and perhaps even more so, ancient $\delta^{13}C_{arc}$ was more strongly influenced by $\delta^{13}C_{carb}$ than $\delta^{13}C_{org}$.

Considering the results provided above, we propose enhanced subduction of C can increase $\delta^{13}C_{carb}$ by increasing $\delta^{13}C_{in}$ due to preferential release of carbonates relative to organic C at arcs. This explains increased $\delta^{13}C_{carb}$ observed in the LE, however it doesn't explain why $\delta^{13}C_{carb}$ returned to around 0‰ (Fig. 1). We propose that the return to "normal" $\delta^{13}C_{carb}$ (~ 0‰) can be explained by delayed release of organic C at intraplate ocean island volcanoes.

Return to normal $\delta^{13}C_{carb}$ via deep recycling of organic C

After releasing carbonates, the slab becomes enriched in organic C, which remains in the slab as refractory graphite/diamond[27,30]. Subducted slabs have been proposed to descend to the core-mantle boundary and reside in “slab graveyards” until being entrained in upwelling mantle plumes, fueling volcanism at ocean islands[31,32]. Upon ascent through the mantle, reduced organic C oxidizes and initiates redox melting[33], allowing organic C to be emitted at ocean islands as CO_2. The large reservoir of Fe^{3+} relative to organic C in the mantle can effectively oxidize organic C without experiencing major changes over geologic time. Unlike arc $\delta^{13}C_{arc}$, $\delta^{13}C_{OIB}$ has received relatively little attention. However, several studies report $\delta^{13}C_{OIB}$, which may support the hypothesis of ocean islands being enriched in organic C.

Figure 3 shows a compilation of $\delta^{13}C_{OIB}$. $\delta^{13}C_{OIB}$ measurements at Kilauea were made on high-temperature volcanic CO_2[34], making them the most appropriate to compare with the arc dataset, which are largely fumarolic measurements. Figure 3 shows that $\delta^{13}C$ at Kilauea is lower than $\delta^{13}C_{arc}$. Measurements made at Koolau[35], Society[23], Loihi[36], and Pitcairn[21] were made on CO_2 from vesicles, glass, or melt inclusions and are subject to isotope fractionation during degassing[37]. For this reason, we identify the least degassed sample from each dataset. Except for Society, which has been shown to have similar noble gas ratios to MORB[23], the least degassed samples from ocean islands have lower $\delta^{13}C$ than MORBs and arcs. These measurements support the possibility of organic C enrichment in ocean island basalts. We propose that delayed release of organic C at ocean islands can explain the return to “normal” $\delta^{13}C_{carb}$ (about 0‰) at the tail-end of the LE. This mechanism requires that subducted organic C retains its low $\delta^{13}C$, which is supported by the observation of light $\delta^{13}C$ values in eclogitic diamonds[38]. Additionally, organic C hosted in subducted oceanic crust may remain physically and chemically isolated from C hosted in ambient mantle precluding any alteration of $\delta^{13}C$ values. Other elements, such as nitrogen, have also been argued to show an enrichment in subducted organic components at ocean island volcanoes[39]. A schematic diagram showing preferential release of organic C at ocean islands and carbonates at arcs shown in Fig. 4.

The proposed mechanism combined with the observation that $\delta^{13}C_{carb}$ has always returned to ~0‰ after large excursions (Fig. 1), leads us to infer that C fluxes into and out of the mantle are at near steady-state with response times to perturbations on the time-scale of mantle transit times, which are on the order of hundreds of million years[40]. If C fluxes into and out of the mantle were out of balance, then due to the more refractory nature of graphitized organic C, we would expect $\delta^{13}C_{carb}$ to increase with time due to the preferential sequestration of light organic C in the mantle. However, $\delta^{13}C_{carb}$ is not observed to increase with time, rather it experiences excursions then returns to ~0‰ (Fig. 1).

Modeling oxygen levels and $\delta^{13}C_{carb}$

Here, we present a carbon-oxygen box model to test whether increased volcanic CO_2 emissions can drive oxygenation and a positive $\delta^{13}C_{carb}$ excursion. The key model assumptions are: 1) Atmospheric oxygen levels are proportional to the mass of organic C in

the system. 2) The mass of organic C buried depends on the flux of carbon deposition, which is proportional to the concentration of atmospheric CO_2:

$$F_w = k \times [CO_{2,\,atm}] \quad (5)$$

where F_w is the flux of CO_2 drawdown from the atmosphere, k is the strength of the weathering feedback, and $[CO_{2,atm}]$ is the concentration of atmospheric CO_2. 3) $\delta^{13}C_{arc}$ is strongly influenced by $\delta^{13}C_{carb}$ and $\delta^{13}C_{OIB}$ by $\delta^{13}C_{org}$. 4) F_{arc} responds to surficial changes in CO_2 fluxes on the order of 10 Myr, while F_{OIB} responds on the order of 100 Myr, corresponding to one mantle transit time for subducted crust[32,40]. These timescales are equivalent to residence times of subducted carbonates and organic C in their respective mantle reservoirs. These residence times appear short compared to those estimated in previous studies (*e.g.*[41]). However, the > 1 billion years residence time of carbon in the mantle is calculated assuming the mantle as a single reservoir for C, which is an oversimplification of the natural C cycle because the mantle contains both recycled and primordial carbon. We assume the residence time of subducted carbonates in the ancient mantle is on the order of 10 million years because they are rapidly released to arc source mantle during subduction[42]. We relate the residence time of organic C to the timescales of mantle convection because organic C is hosted as refractory/graphite diamond in subducted oceanic crust and is unlikely to efficiently mix with surrounding mantle. Therefore, as soon as the subducted oceanic crust completes a convective cycle and undergoes partial melting in the oxidized upper mantle, organic C will be efficiently degassed as CO_2.

Figure 5 was generated by increasing mid-ocean ridge CO_2 emissions by 1000-fold instantaneously at 2.5 Ga. Figure 5 demonstrates that in response to increased CO_2 emissions, the production flux of carbonates and organic C increases, causing atmospheric oxygen to increase immediately due to the increased reservoir of buried organic C. Shortly after oxygen increases, $\delta^{13}C_{carb}$ increases as $\frac{F_{arc}}{F_{tot}}$ increases, with the delay being dictated by the time required for carbonate to be deposited, subducted, and released at arcs as CO_2 (Fig. 5). After a longer delay, dictated by the time required for organic C to be buried and later released as CO_2 at ocean islands, $\delta^{13}C_{carb}$ decreases in response to increased $\frac{F_{OIB}}{F_{tot}}$. Note that model results were generated keeping f_{org} constant at 0.20 throughout the model run.

A notable result of the model is that simply increasing volcanic CO_2 emissions can match the magnitude of oxygen increase while nearly matching the magnitude of $\delta^{13}C$ excursions observed for the GOE and LE, which can't be achieved by solely changing f_{org}[43,44]. Another notable result of the model is that it closely reproduces the topology of the Lomagundi event, which displays a gradual increase in $\delta^{13}C$ and terminates abruptly with $\delta^{13}C$ rapidly decreasing to ~0‰. Supplementary Fig. 2 shows how varying different model parameters affects the shape and magnitude of the C isotope excursion. Furthermore, the present model shows that a permanent transition to increased volcanic CO_2 emissions produces a permanent transition to higher atmospheric O_2 but causes a transient excursion in $\delta^{13}C$ as observed in natural data. We note that our model is consistent with any event that increases CO_2 emissions. Therefore, the proposed mechanism is not only applicable to the Great

Oxidation and Lomagundi event (see Supp. Fig. 3), it can also explain other large oxidation and C isotope excursions such as the events observed at the end of the Proterozoic[1], which have also been proposed to result from large emissions of CO_2[45]. This is in contrast to the model of Duncan and Dasgupta[27], which relies on initiation of plate tectonics to coincide with the GOE.

In summary, we propose that the GOE and LE can be explained by a single mechanism – increased carbonate and organic C deposition driven by enhanced volcanic CO_2 degassing, possibly driven by a transition from stagnant/sluggish lid to plate tectonics[12]. Alternatively, the rapid emergence of subaerial continents[15] or global glaciation[17,24], proposed to have occurred ~2.5–2.3 Ga, have been argued to facilitate enhanced volcanic CO_2 emissions by supplying sediments to convergent margins thereby facilitating more efficient subduction and related volcanism[17]. The presented hypothesis is consistent with natural observations such as contemporaneous increases in continental weathering[24], heavy $\delta^{13}C_{arc}$[22], and possible light $\delta^{13}C_{OIB}$[21]. We present a carbon-oxygen model which demonstrates increased volcanic CO_2 emissions coupled with preferential release of carbonate-derived CO_2 at arc volcanoes and the delayed release of organic C at ocean island volcanoes can drive atmospheric oxygenation and positive C isotope excursions without requiring any changes to f_{org}

The present study raises several important implications. 1) Large-scale, long-lived positive $\delta^{13}C$ isotope excursions such as the LE do not require changes in f_{org}, they may be the result of fractionation of carbonates and organic C in Earth's interior. 2) Oxygen and biomass production may be controlled by tectonic conditions dictating volcanic CO_2 emissions. 3) Carbon fluxes into and out of the mantle may be close to steady state, with response times to perturbations on the order of mantle transit times. These conclusions provide an alternate interpretation of the evolution of CO_2 and O_2 on Earth and can inform our thinking on how Earth, the only known inhabited planet in our Solar System and beyond, became and remained oxygenated, allowing for the proliferation of complex life on the surface.

Methods

Quantifying C release from the subducting slab

To quantify carbon release from the subducting slab via metamorphic decarbonation, we performed thermodynamic calculations with the software package *Perple_X*[50]. We calculate the stable mineral assemblage of a model carbonated pelite as a function of pressure and temperature, with a bulk composition from Tsuno et al.[29]. We use the calculated bulk composition of the residual solid lithology to determine the amount of CO_2 that can be retained in the solid lithology in the form of carbonates. The CO_2 wt.% of the bulk rock decreases as P and T increase (Fig. 2a). We then calculate how much of the original carbon is retained in the solid lithology along subduction zone P-T paths relevant to ancient subduction zones. Following the arguments of Duncan and Dasgupta[27] we assume that ancient subduction zones were hotter than those in the present day by about 70 °C/Gyr. Therefore, to investigate conditions relevant to the GOE and LE, we increased the temperatures of slab top P-T paths from Syracuse et al.[51] by 175 °C. Assuming a starting

CO_2 of 5 wt.% as mineral carbonates, the amount of original subducted CO_2 retained in the slab as carbonate was calculated along *P-T* paths according using the following equation:

$$\text{Percent } CO_2 \text{ retained} = \frac{5 - CO_2 \text{ wt\% of bulk rock}}{5} \times 100 \quad (6)$$

Where 5 is the initial amount of CO_2 in the bulk rock composition in wt%, and 'CO_2 wt% of bulk rock' is the CO_2 content of the bulk calculated as a function of pressure and temperature using *Perple_X*.

We note that the extent of metamorphic decarbonation calculated in this fashion provides an underestimate if extraneous fluid source is available. Incorporating open system, fluid infiltration induced metamorphic decarbonation more efficiently breaks down carbonates in the slab[52]. Similarly, the availability of extraneous fluid allows carbonate dissolution to be an important process of carbonate removal[42]. Furthermore, for warm subduction zones of ancient past, complete carbonate removal from the downgoing slab likely took place via carbonated melting[53]. Hence there are several mechanisms that could have led to complete exhaustion of carbonates from the slab in ancient subduction zones.

To quantify graphitized organic carbon release from subducting slabs we followed the methods of Duncan and Dasgupta[27], in which the authors predict dissolved CO_2 concentrations in hydrous rhyolitic melts in equilibrium with graphite/diamond as a function of *P, T,* and fO_2. In our calculations of graphite/diamond dissolution in silicate melts we use the same *P-T* paths described above and fO_2 was calculated along the CCO buffer[54]. Organic C removal efficiency would be even lower if more reduced slab conditions are used, *i.e.,* the fO_2 conditions used give the highest CO_2 dissolution capacity and graphite/diamond saturation. The results shown in Fig. 2 were generated assuming 1 wt% graphite in the initial bulk composition. See Duncan and Dasgupta[27] for more details on calculations.

Modeling atmospheric oxygen levels and $\delta^{13}C$ of carbonates

We developed a new coupled carbon-oxygen cycle model which tracks $\delta^{13}C$. The model tracks how a set of carbon reservoirs (C_i) respond to changes in carbon fluxes (F_i) between these reservoirs. The surface reservoirs are the atmosphere-ocean (C_{atm}), solid carbonates (C_{carb}), and organic carbon (C_{org}), which are generated from the atmospheric reservoir (in this model we do not treat any fractionations between the ocean-atmosphere reservoirs). The transfer of carbon from the atmosphere-ocean reservoir into the carbonate and organic carbon reservoirs is controlled by a weathering flux (F_w, which is divided into F_{carb} and F_{org}) which is proportional to the weathering constant (k) and the concentration of CO_2 in the atmosphere (C_{atm}). Carbon that is fluxed out of the atmosphere can be deposited as either carbonates or organic carbon. In Fig. 5 we prescribe that 40% of carbonates and organic C fluxed out of the atmosphere are added to a crustal reservoir (C_{carb} and C_{org}), while the other 60% are subducted (χ =0.60). To demonstrate that a carbon isotope excursion is possible without changing the fraction of organic C buried relative to carbonate, we hold f_{org} constant at 0.20 throughout the model.

While treating carbon in the Earth's interior, we divide the mantle into three different carbon reservoirs. The first reservoir holds primitive carbon C_{prm}, which we treat as having existed in the mantle since its formation, additionally it receives no contribution from subducted components throughout the model evolution. The other two mantle carbon reservoirs consist of carbon hosted in subducted carbonate (C_{mcarb}), and carbon hosted in organic carbon (C_{morg}), which have influxes from surfaces reservoirs controlled by the flux of subducted carbonate (F_{subc}) and organic carbon (F_{subo}) respectively. To relate oxygen levels to the carbon cycle we assume the atmospheric oxygen levels are directly proportional to the mass of organic carbon in the surface and mantle reservoirs.

We prescribe that subducted carbon can leave the mantle reservoirs via arc volcanoes (F_{arc}) and ocean island volcanoes (F_{OIB}). In order to keep track of how differential release of carbonates versus organics at different volcanic settings affects C isotopes of CO_2 emissions through time, we treat volcanic CO_2 fluxes at arc volcanoes and ocean island volcanoes as the sum of CO_2 fluxes derived from carbonates (F_{arcc} & F_{OIBc}), organic carbon (F_{arco} & F_{OIBo}), and primitive mantle carbon (F_{arcp} & F_{OIBp}), each having their own distinct $\delta^{13}C$. To account for the differential release of carbonates and organics at arcs and OIBs we prescribe that a certain fraction of subducted carbonates (α_{carb}) and organics (α_{org}) are released at arcs, with the remaining fraction released at OIBs (1- α_{carb}, and 1- α_{org}). In accordance with our calculations in the main text (Fig. 2), we treat carbonates as being completely released at arcs ($\alpha_{carb} = 1$), and organics as being completed released at OIBs ($\alpha_{org} = 0$) when generating Fig. 5. Supplementary Figs. 2 and 3 show how probable variations in α_{carb} and α_{org} would influence the modeled evolution of $\delta^{13}C_{carb}$.

Subducted carbon cycled through the mantle and released at arc volcanoes travel on the order of hundreds of kilometers, while carbon cycled through ocean island volcanoes may travel to the core-mantle boundary, traveling distances on the order of thousands of kilometers. Assuming mantle convection occurs on the order of 1 cm/yr the residence time of mantle carbon released at arcs (τ_{arc}) is on the order of 10 Myr, while the residence time of mantle carbon released at ocean island volcanoes (τ_{OIB}) is on the order of 100 Myr. Therefore, perturbations to subduction carbon fluxes will manifest themselves in arc volcanoes before ocean island volcanoes. The total volcanic CO_2 outgassing flux (F_{out}) is a sum of the fluxes at arcs, OIBs, and MORB.

The system of equations representing this coupled surface and interior carbon cycle are:

$$\frac{dC_{atm}}{dt} = F_{out} - F_{w} \tag{7}$$

$$\frac{dC_{carb}}{dt} = (1 - f_{org})F_{w} - F_{subc} \tag{8}$$

$$\frac{dC_{org}}{dt} = f_{org}F_{w} - F_{subo} \tag{9}$$

$$\frac{d\mathrm{C}_{\mathrm{mcarb}}}{dt} = F_{\mathrm{subc}} - F_{\mathrm{arcc}} - F_{\mathrm{oibc}} \quad (10)$$

$$\frac{d\mathrm{C}_{\mathrm{morg}}}{dt} = F_{\mathrm{subo}} - F_{\mathrm{arco}} - F_{\mathrm{oibo}} \quad (11)$$

$$\frac{d\mathrm{C}_{\mathrm{prm}}}{dt} = -(F_{\mathrm{OIBp}} + F_{\mathrm{MORB}}) \quad (12)$$

$$\mathrm{O}_{\mathrm{atm}} = \mathrm{C}_{\mathrm{org}} + \mathrm{C}_{\mathrm{morg}} \quad (13)$$

$$F_{\mathrm{w}} = k\mathrm{C}_{\mathrm{atm}} \quad (14)$$

$$F_{carb} = F_{w}(1 - f_{\mathrm{org}}) \quad (15)$$

$$F_{org} = F_{\mathrm{w}}(f_{\mathrm{org}}) \quad (16)$$

$$F_{\mathrm{subc}} = \chi F_{\mathrm{carb}} \quad (17)$$

$$F_{\mathrm{subo}} = \chi F_{\mathrm{org}} \quad (18)$$

$$F_{\mathrm{arc}} = F_{\mathrm{arcc}} + F_{\mathrm{arco}} \quad (19)$$

$$F_{\mathrm{arcc}} = \alpha_{\mathrm{carb}} F_{\mathrm{subc}} \quad (20)$$

$$F_{\mathrm{arco}} = \alpha_{\mathrm{org}} F_{\mathrm{subo}} \quad (21)$$

$$F_{\mathrm{OIB}} = F_{\mathrm{OIBc}} + F_{\mathrm{OIBo}} + F_{\mathrm{OIBp}} \quad (22)$$

$$F_{\mathrm{OIBc}} = (1 - \alpha_{\mathrm{carb}}) F_{\mathrm{subo}} \quad (23)$$

$$F_{\mathrm{OIBo}} = (1 - \alpha_{\mathrm{org}}) F_{\mathrm{subo}} \quad (24)$$

$$F_{\mathrm{OIBp}} = \kappa_1 \tag{25}$$

$$F_{\mathrm{MORB}} = \kappa_2 \tag{26}$$

$$F_{\mathrm{out}} = F_{\mathrm{OIB}} + F_{\mathrm{MORB}} + F_{\mathrm{arc}} \tag{27}$$

A main focus of the model is to demonstrate how $\delta^{13}C_{carb}$ evolves in response to perturbations to carbon fluxes. Therefore, we track the $\delta^{13}C$ evolution of different carbon reservoirs and fluxes with the following set of equations:

$$\delta^{13}C_{\mathrm{atm}}(t) = \frac{F_{\mathrm{OIB}}}{F_{\mathrm{out}}}\delta^{13}C_{\mathrm{OIB}}(t) + \frac{F_{\mathrm{arc}}}{F_{\mathrm{out}}}\delta^{13}C_{\mathrm{arc}}(t) + \frac{F_{\mathrm{MORB}}}{F_{\mathrm{out}}}\delta^{13}C_{\mathrm{MORB}}(t) \tag{28}$$

$$\delta^{13}C_{\mathrm{OIB}}(t) = \frac{F_{\mathrm{OIBc}}}{F_{\mathrm{OIB}}}\delta^{13}C_{\mathrm{carb}}(t-\tau_{\mathrm{OIB}}) + \frac{F_{\mathrm{OIBo}}}{F_{\mathrm{OIB}}}\delta^{13}C_{\mathrm{org}}(t-\tau_{\mathrm{OIB}}) + \frac{F_{\mathrm{OIBp}}}{F_{\mathrm{OIB}}}\delta^{13}C_{\mathrm{prm}} \tag{29}$$

$$\delta^{13}C_{\mathrm{arc}}(t) = \frac{F_{\mathrm{arcc}}}{F_{\mathrm{arc}}}\delta^{13}C_{\mathrm{carb}}(t-\tau_{\mathrm{arc}}) + \frac{F_{\mathrm{arco}}}{F_{\mathrm{arc}}}\delta^{13}C_{\mathrm{org}}(t-\tau_{\mathrm{arc}}) \tag{30}$$

$$\delta^{13}C_{\mathrm{carb}}(t) = \delta^{13}C_{\mathrm{atm}}(t) + 5 \tag{31}$$

$$\delta^{13}C_{\mathrm{org}}(t) = \delta^{13}C_{\mathrm{atm}}(t) - 20 \tag{32}$$

where $\delta^{13}C_i(t)$ is the $\delta^{13}C_i$ value for carbon reservoir or flux i at time *t*, with atm = atmospheric reservoir, carb = carbonate reservoir, org = organic carbon reservoir, prm = primitive mantle reservoir, arc = arc flux, and OIB = ocean island flux, and MORB = mid-ocean ridge flux. We set $\delta^{13}C_{prm}$ to a constant value of −5‰ for the duration of the model, as we have assumed it has no influx of carbon from the surface reservoirs. The equations for $\delta^{13}C_{crb}(t)$ and $\delta^{13}C_{org}(t)$ are offset from $\delta^{13}C_{atm}(t)$ by +5 and −20 respectively because we assume that $\Delta^{13}C_{crb\text{-}org}$ = 25‰ and f_{org} = 0.20.

The model run to generate Fig. 5 was designed to simulate increased CO_2 emissions. To simulate this scenario, the model was run with the initial conditions given in supplementary Table 1. After evolving with no perturbations for 1 billion years, we prescribed that MORB emissions increase from 10^{13} to 10^{16} g C/Myr. In order to check whether the model is an acceptable representation of the global C cycle model we increased MORB emissions a

second time to 10^{19} g C/Myr (similar to present day estimates[41]), and model-dependent reservoir sizes and fluxes are in line with present day estimates (Supp. Fig. 3). The increased CO_2 emissions cause increased deposition of carbonates and organic C, which drives increased subduction fluxes of both carbonates and organic C. The increased subduction flux of C coupled with the differential release of carbonates and organics at different volcanic settings described above results in increased oxygen levels and the positive C isotope excursion shown in Fig. 5.

Supplementary Material

Refer to Web version on PubMed Central for supplementary material.

Acknowledgements

The authors thank Jeremy Caves and an anonymous reviewer for their constructive reviews. R.D acknowledges support from an NSF grant OCE-1338842, NASA grant 80NSSC18K0828, and the Deep Carbon Observatory. J.E. acknowledges support from a NASA Postdoctoral Program fellowship with the NASA Astrobiology Institute.

References

1. Lyons TW, Reinhard CT & Planavsky NJ The rise of oxygen in Earth's early ocean and atmosphere. Nature 506, 307–315 (2014). [PubMed: 24553238]
2. Luo G et al. Rapid oxygenation of Earth's atmosphere 2.33 billion years ago. Sci. Adv 2, e1600134 (2016). [PubMed: 27386544]
3. Bekker A, Karhu JA & Kaufman AJ Carbon isotope record for the onset of the Lomagundi carbon isotope excursion in the Great Lakes area, North America. Precambrian Res. 148, 145–180 (2006).
4. Karhu JA & Holland HD Carbon isotopes and the rise of atmospheric oxygen. Geology 24, 867–870 (1996).
5. Planavsky NJ et al. Evidence for oxygenic photosynthesis half a billion years before the Great Oxidation Event. Nat. Geosci 7, 283–286 (2014).
6. Kasting JF What caused the rise of atmospheric O2? Chem. Geol 362, 13–25 (2013).
7. Bekker A et al. Dating the rise of atmospheric oxygen. Nature 427, 117–120 (2004). [PubMed: 14712267]
8. Bekker A et al. Fractionation between inorganic and organic carbon during the Lomagundi (2.22–2.1 Ga) carbon isotope excursion. Earth Planet. Sci. Lett 271, 278–291 (2008).
9. Kump LR & Barley ME Increased subaerial volcanism and the rise of atmospheric oxygen 2.5 billion years ago. Nature 448, 1033–1036 (2007). [PubMed: 17728754]
10. Lee C-TA et al. Two-step rise of atmospheric oxygen linked to the growth of continents. Nat. Geosci 9, 417–424 (2016).
11. Holland HD Why the atmosphere became oxygenated: A proposal. Geochim. Cosmochim. Acta 73, 5241–5255 (2009).
12. Condie KC, Aster RC & Van Hunen J A great thermal divergence in the mantle beginning 2.5 Ga: Geochemical constraints from greenstone basalts and komatiites. Geosci. Front 7, 543–553 (2016).
13. Korenaga J Initiation and evolution of plate tectonics on Earth: theories and observations. Annu. Rev. Earth Planet. Sci 41, 117–151 (2013).
14. Fuentes JJ, Crowley JW, Dasgupta R & Mitrovica JX The influence of plate tectonic style on melt production and CO_2 outgassing flux at mid-ocean ridges. Earth Planet. Sci. Lett 511, 154–163 (2019).
15. Bindeman IN et al. Rapid emergence of subaerial landmasses and onset of a modern hydrologic cycle 2.5 billion years ago. Nature 557, 545–548 (2018). [PubMed: 29795252]
16. Gumsley AP et al. Timing and tempo of the Great Oxidation Event. Proc. Natl. Acad. Sci 114, 1811–1816 (2017). [PubMed: 28167763]

17. Sobolev SV & Brown M Surface erosion events controlled the evolution of plate tectonics on Earth. Nature 570, 52–57 (2019). [PubMed: 31168102]
18. Moussallam Y, Oppenheimer C & Scaillet B On the relationship between oxidation state and temperature of volcanic gas emissions. Earth Planet. Sci. Lett 520, 260–267 (2019).
19. Campbell IH & Allen CM Formation of supercontinents linked to increases in atmospheric oxygen. Nat. Geosci 1, 554–558 (2008).
20. Marty B & Zimmermann L Volatiles (He, C, N, Ar) in mid-ocean ridge basalts: assesment of shallow-level fractionation and characterization of source composition. Geochim. Cosmochim. Acta 63, 3619–3633 (1999).
21. Aubaud C, Pineau F, Hékinian R & Javoy M Carbon and hydrogen isotope constraints on degassing of CO_2 and H_2O in submarine lavas from the Pitcairn hotspot (South Pacific). Geophys. Res. Lett. 33, L02308 (2006).
22. Mason E, Edmonds M & Turchyn AV Remobilization of crustal carbon may dominate volcanic arc emissions. Science 357, 290–294 (2017). [PubMed: 28729507]
23. Aubaud C, Pineau F, Hékinian R & Javoy M Degassing of CO_2 and H_2O in submarine lavas from the Society hotspot. Earth Planet. Sci. Lett 235, 511–527 (2005).
24. Keller CB et al. Neoproterozoic glacial origin of the Great Unconformity. Proc. Natl. Acad. Sci 116, 1136–1145 (2019). [PubMed: 30598437]
25. Avanzinelli R, Casalini M, Elliott T & Conticelli S Carbon fluxes from subducted carbonates revealed by uranium excess at Mount Vesuvius, Italy. Geology 46, 259–262 (2018).
26. Sano Y & Marty B Origin of carbon in fumarolic gas from island arcs. Chem. Geol 119, 265–274 (1995).
27. Duncan MS & Dasgupta R Rise of Earth's atmospheric oxygen controlled by efficient subduction of organic carbon. Nat. Geosci 10, 387–392 (2017).
28. Buseck PR & Beyssac O From organic matter to graphite: graphitization. Elements 10, 421–426 (2014).
29. Tsuno K, Dasgupta R, Danielson L & Righter K Flux of carbonate melt from deeply subducted pelitic sediments: Geophysical and geochemical implications for the source of Central American volcanic arc. Geophys. Res. Lett 39, L16307 (2012).
30. Galvez ME et al. Graphite formation by carbonate reduction during subduction. Nat. Geosci 6, 473–477 (2013).
31. Hofmann AW & White WM Mantle plumes from ancient oceanic crust. Earth Planet. Sci. Lett 57, 421–436 (1982).
32. Li M & McNamara AK The difficulty for subducted oceanic crust to accumulate at the Earth's core-mantle boundary. J. Geophys. Res. Solid Earth 118, 1807–1816 (2013).
33. Stagno V, Ojwang DO, McCammon CA & Frost DJ The oxidation state of the mantle and the extraction of carbon from Earth's interior. Nature 493, 84–88 (2013). [PubMed: 23282365]
34. Gerlach TM & Taylor BE Carbon isotope constraints on degassing of carbon dioxide from Kilauea Volcano. Geochim. Cosmochim. Acta 54, 2051–2058 (1990).
35. Hauri E SIMS analysis of volatiles in silicate glasses, 2: isotopes and abundances in Hawaiian melt inclusions. Chem. Geol 183, 115–141 (2002).
36. Exley RA, Mattey DP, Clague DA & Pillinger CT Carbon isotope systematics of a mantle 'hotspot': a comparison of Loihi Seamount and MORB glasses. Earth Planet. Sci. Lett 78, 189–199 (1986).
37. Holloway J & Blank J Application of experimental results to C-O-H species in natural melts. Reviews in Mineralogy and Geochemistry 30, 187–230 (1994).
38. Shirey SB et al. Diamonds and the Geology of Mantle Carbon. Rev. Mineral. Geochemistry 75, 355–421 (2013).
39. Marty B & Dauphas N The nitrogen record of crust–mantle interaction and mantle convection from Archean to Present. Earth Planet. Sci. Lett 206, 397–410 (2003).
40. Christensen UR & Hofmann AW Segregation of subducted oceanic crust in the convecting mantle. J. Geophys. Res. Solid Earth 99, 19867–19884 (1994).

41. Dasgupta R & Hirschmann MM The deep carbon cycle and melting in Earth's interior. Earth Planet. Sci. Lett 298, 1–13 (2010).
42. Kelemen PB & Manning CE Reevaluating carbon fluxes in subduction zones, what goes down, mostly comes up. Proc. Natl. Acad. Sci. 112, E3997–E4006 (2015). [PubMed: 26048906]
43. Krissansen-Totton J, Buick R & Catling DC A statistical analysis of the carbon isotope record from the Archean to phanerozoic and implications for the rise of oxygen. Am. J. Sci 315, 275–316 (2015).
44. Olson SL et al. Volcanically modulated pyrite burial and ocean–atmosphere oxidation. Earth Planet. Sci. Lett 506, 417–427 (2019).
45. Williams JJ, Mills BJW & Lenton TM A tectonically driven Ediacaran oxygenation event. Nat. Commun 10, 2690 (2019). [PubMed: 31217418]
46. Liu X-M et al. Tracing Earth's O2 evolution using Zn/Fe ratios in marine carbonates. Geochemical Perspect. Lett 2, 24–34 (2016).
47. Condie KC & Aster RC Episodic zircon age spectra of orogenic granitoids: The supercontinent connection and continental growth. Precambrian Res. 180, 227–236 (2010).
48. Clift PD A revised budget for Cenozoic sedimentary carbon subduction. Rev. Geophys 55, 97–125 (2017).
49. Carter LB & Dasgupta R Decarbonation in the Ca-Mg-Fe carbonate system at mid-crustal pressure as a function of temperature and assimilation with arc magmas – Implications for long-term climate. Chem. Geol 492, 30–48 (2018).

References

50. Connolly JAD The geodynamic equation of state: What and how. Geochemistry, Geophys. Geosystems 10, Q10014 (2009).
51. Syracuse EM et al. The global range of subduction zone thermal models. Phys. Earth Planet. Inter 183, 73–90 (2010).
52. Gorman PJ, Kerrick DM & Connolly JAD Modeling open system metamorphic decarbonation of subducting slabs. Geochemistry, Geophys. Geosystems 7, Q04007 (2006).
53. Dasgupta R Ingassing, storage, and outgassing of terrestrial carbon through geologic time. Rev. Mineral. Geochemistry 75, 183–229 (2013).
54. Frost DJ & Wood BJ Experimental measurements of the fugacity of CO_2 and graphite/diamond stability from 35 to 77 kbar at 925 to 1650°C. Geochim. Cosmochim. Acta 61, 1565–1574 (1997).

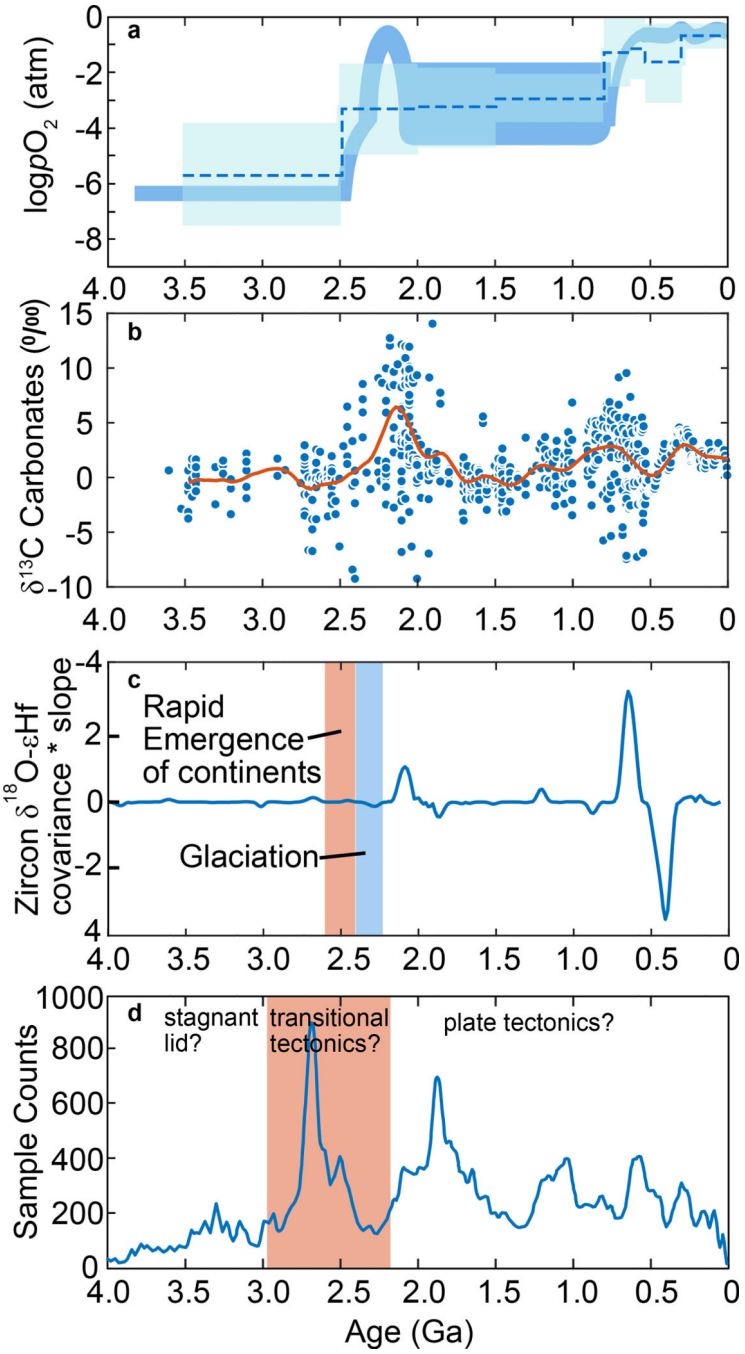

Figure 1. Variations in atmospheric O_2, $\delta^{13}C$ of carbonates, and tracers of tectonic processes through geologic time.

a, Qualitative model of atmospheric O_2 (solid blue curve)[1] and estimation of atmospheric O_2 from Zn/Fe ratios in carbonates (dashed blue line with shaded region for uncertainties)[46]. **b**, Carbonate $\delta^{13}C$ through time[43]. **c,** Zircon $\delta^{18}O$-εHf covariance*slope from Keller, et al.[24], where positive values indicate increases in crustal contribution to magmatism. Orange band is proposed timing for rapid emergence of subaerial continents inferred from triple-oxygen isotopes[15], blue band is timing large-scale glaciations[24].**d,** U/Pb age distribution of detrital

and orogenic zircons[47], with orange band showing the proposed timing of transitional tectonics between stagnant lid and plate tectonics[12].

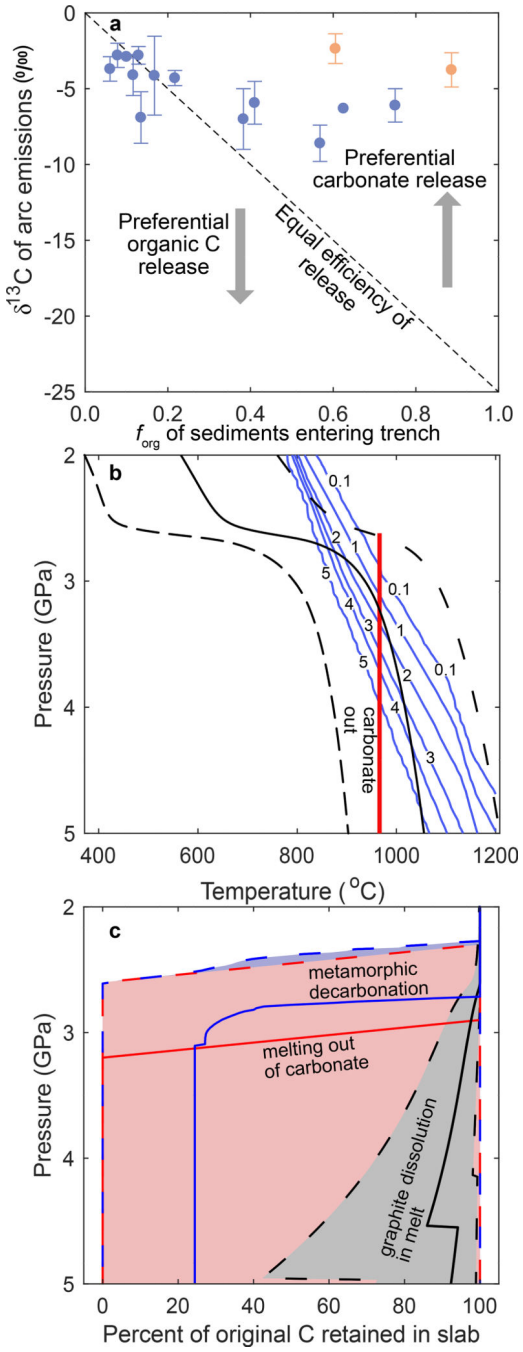

Figure 2. Natural data and petrologic calculations suggesting preferential release of carbonate over organic carbon in present-day and ancient subduction zones.

a, $\delta^{13}C_{arc}$[22] versus f_{org} of sediments at modern subduction zones[48]. Orange symbols represent volcanoes erupting through carbonates, increasing likelihood of crustal carbonate dominating $\delta^{13}C_{arc}$[49]. Dashed line shows equal efficiency of release for carbonates and organic C. Error bars are 1σ. **b**, Ancient slab *P-T* paths[27] (Dashed black lines are cold and hot *P-T* paths, solid black line is average of the two) compared to metamorphic decarbonation (blue lines labeled with wt% CO_2 retained in slab), and melting out of carbonates[29] (red line). **c**, Percentage of C retained in slab versus depth. Blue lines show

how much C remains in slab (solid and dashed lines calculated along respective *P-T* paths of **b**) during metamorphic decarbonation. Red lines calculated for carbonates released by carbonated melting (red line in **b**). Black lines for organic C release by graphite dissolution in silicate melts.

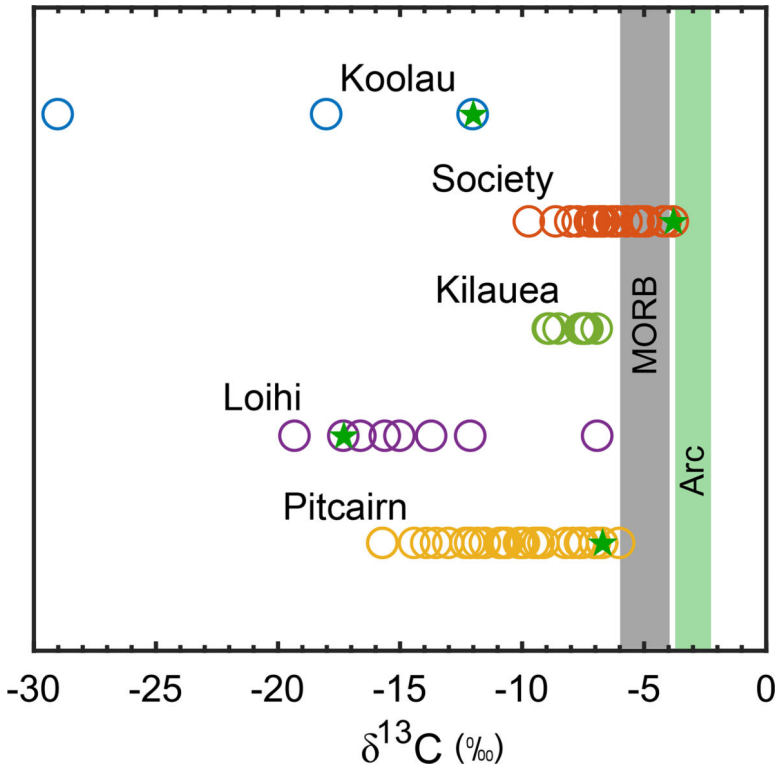

Figure 3. Comparison of carbon isotope compositions of CO_2 emissions from different volcanic settings.

Measurements made on samples from Koolau[35], Society[23], Loihi[36], and Pitcairn[21] were made on CO_2 from vesicles, glass, or melt inclusions and are therefore subject to isotope fractionation during degassing[37]. Least degassed samples are marked for each location with a green star. Measurements at Kilauea[34] are made on high-*T* volcanic gas emissions and are therefore the most directly applicable for comparison to the global flux-weighted average of arc CO_2 emissions[22]. Available data suggests that ocean islands may emit CO_2 with lower $\delta^{13}C$ than MORB and arcs.

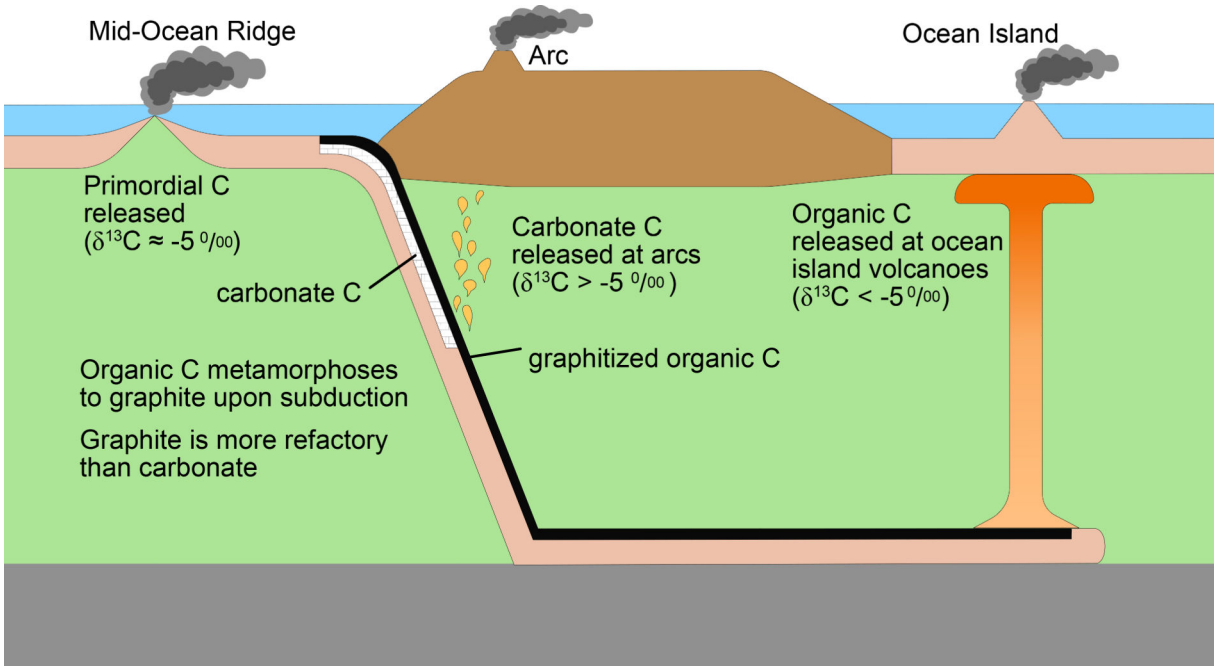

Figure 4. Schematic diagram showing preferential release of carbonate C at arc volcanoes and organic C at ocean island volcanoes.

Both carbonates and organic carbon are deposited on the seafloor and subducted into Earth's interior. Upon subduction, organic C metamorphoses to graphite, which is more refractory than carbonate. At subarc conditions carbonates are preferentially released from the slab (Fig. 2) relative to graphitized organic C, increasing arc volcano $\delta^{13}C$ to values greater than −5‰. Graphitized organic C remains in slab and is transported deep into the mantle, where it may become entrained in upwelling mantle plumes feeding ocean island volcanoes. Upwelling, reduced organic C likely undergoes redox melting, decreasing ocean island volcano $\delta^{13}C$ to <−5‰.

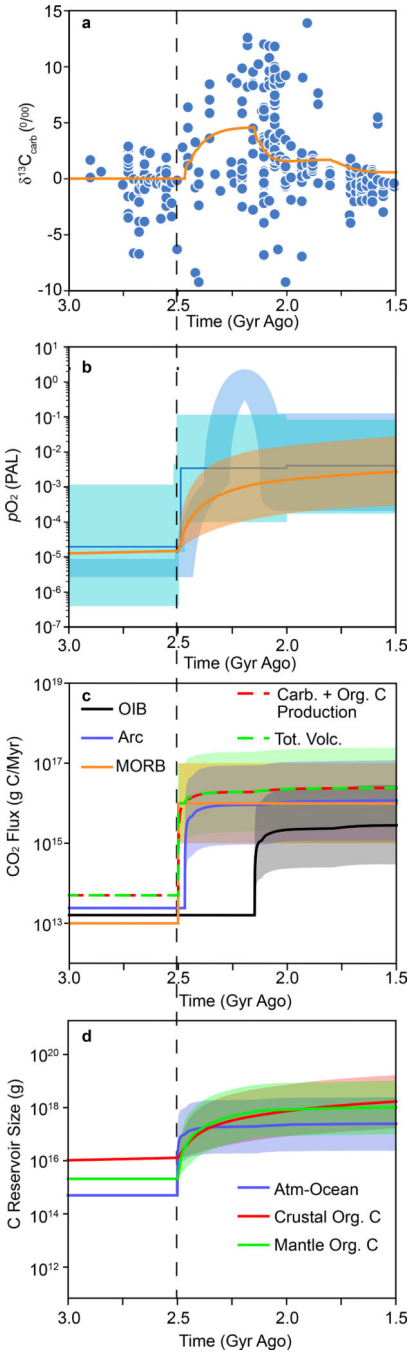

Figure 5. Model results showing how tectonically-driven increased CO_2 emissions and deep recycling of organic C can drive GOE and LE.

a. $\delta^{13}C_{carb}$ versus time. Orange curve is model result, blue symbols are natural data. When increases to MOR CO_2 emissions are large, magnitude of C isotope excursion becomes insensitive to magnitude of changes to MOR CO_2 emissions (See SI). **b**. Atmospheric O_2 versus time. Orange curve shows results for 1000-fold increase in MOR CO_2 emissions, while bands show results when increases range from 100-fold to 10,000-fold. Blue curves from Fig. 1. Vertical dashed line emphasizes that oxygen increases before C isotope

excursion. **c**. CO_2 fluxes versus time. Shaded regions as in **b**. **d**. C reservoir size versus time. Shaded regions as in **b**.